# Anticancer Activity Expressed by a Library of 2,9-Diazaperopyrenium Dications

Karel J. Hartlieb,[†] Leah S. Witus,[†] Daniel P. Ferris,[†] Ashish N. Basuray,[†] Mohammed M. Algaradah,[‡] Amy A. Sarjeant,[†] Charlotte L. Stern,[†] Majed S. Nassar,[‡] Youssry Y. Botros,[§] and J. Fraser Stoddart*,[†]

[†]Department of Chemistry, Northwestern University, 2145 Sheridan Road, Evanston, Illinois 60208, United States, [‡]Joint Center of Excellence in Integrated Nano-Systems (JCIN), King Abdul-Aziz City for Science and Technology (KACST), P.O. Box 6068, Riyadh 11442, Kingdom of Saudia Arabia, and [§]University Research Office, Intel Corporation, Building RNB-6-61, 2200 Mission College Boulevard, Santa Clara, California 95054, United States

ABSTRACT
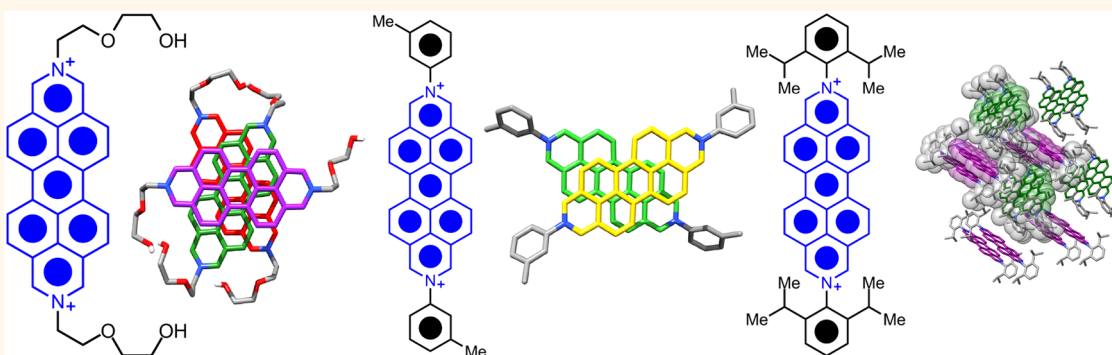
Polyaromatic compounds are well-known to intercalate DNA. Numerous anticancer chemotherapeutics have been developed upon the basis of this recognition motif. The compounds have been designed such that they interfere with the role of the topoisomerases, which control the topology of DNA during the cell-division cycle. Although many promising chemotherapeutics have been developed upon the basis of polyaromatic DNA intercalating systems, these candidates did not proceed past clinical trials on account of their dose-limiting toxicity. Herein, we discuss an alternative, water-soluble class of polyaromatic compounds, the 2,9-diazaperopyrenium dications, and report *in vitro* cell studies for a library of these dications. These investigations reveal that a number of 2,9-diazaperopyrenium dications show similar activities as doxorubicin toward a variety of cancer cell lines. Additionally, we report the solid-state structures of these dications, and we relate their tendency to aggregate in solution to their toxicity profiles. The addition of bulky substituents to these polyaromatic dications decreases their tendency to aggregate in solution. The derivative substituted with 2,6-diisopropylphenyl groups proved to be the most cytotoxic against the majority of the cell lines tested. In the solid state, the 2,6-diisopropylphenyl-functionalized derivative does not undergo $\pi \cdots \pi$ stacking, while in aqueous solution, dynamic light scattering reveals that this derivative forms very small (50−100 nm) aggregates, in contrast with the larger ones formed by dications with less bulky substituents. Alteration of the aromaticitiy in the terminal heterocycles of selected dications reveals a drastic change in the toxicity of these polyaromatic species toward specific cell lines.

KEYWORDS: anticancer activity · diazaperopyrenium dications · DNA intercalation

O ne of the major strategies employed in cancer chemotherapy[1,2] is the use of small molecules that disrupt DNA replication and so halt rapid cellular division and promote cell apoptosis. To this end, molecules that intercalate double-stranded DNA have shown promise as anticancer agents often as a result of the inhibition of topoisomerase enzymes.[3−5] Intercalating compounds include ethidium bromide,[6−11] proflavine[11−16] and doxorubicin,[3,17−22] the last of which has been approved clinically and is administered as the hydrochloride salt in the clinic to treat a variety of cancers. Although effective as a chemotherapeutic agent, prolonged therapeutic regiments using doxorubicin lead to serious adverse implications[17,22] for the cardiovascular system, the most significant[17] of which is cardiomyopathy. Continuing

efforts, therefore, to uncover alternative drug candidates for anticancer treatments to improve upon established therapeutics remains a top priority in the eyes of medicinal chemists. From these continuing efforts, other DNA-intercalating drug candidates, such as Mitonafide[23,24] and Amodafide[25,26] and the bis-intercalating Elinafide,[27−30] have been identified[31−33] and shown to be highly cytotoxic to cancer cells. After numerous clinical studies[29] of these candidates, however, many compounds have yet to be developed as chemotherapeutic agents on account of their dose-limiting toxicity. In order to develop new drugs that follow the established DNA-intercalation pathway, and yet have different pharmacokinetics, we need to find out more about the physical properties of the drug candidates. The most common structural feature of these DNA intercalators is the presence of a planar aromatic region to aid and abet stacking in between the DNA bases. Although there are many examples of anticancer drug candidates, such as naphthalene diimide-based compounds,[33] containing extended aromatic regions, their low solubilities in aqueous solutions have often limited anticancer therapeutic-based applications. Molecules which contain an aromatic region, while remaining water-soluble, are particularly promising drug candidates. These two properties are especially true for cationic DNA intercalators, since investigations[34,35] have shown that electrostatic interactions with the negatively charged phosphate backbone of DNA can leverage attractive Coulombic intercalation interactions.

Recently, we have been investigating[36−39] the materials properties of the N,N'-dimethyl-2,9-diazaperopyrenium dication (dimethyl-DAPP^{2+}), which has (Figure 1) an extended, electron-rich aromatic core region flanked on either side by electron-deficient pyridinium rings. This compound has found use in mechanically interlocked molecules[36] (MIMs), graphene exfoliation applications,[39] and in host−guest inclusion complexes.[37,38] The aqueous solubility, imparted by the dicationic nature of this compound, led us to consider whether the extended aromatic region present in dimethyl-DAPP^{2+} and related compounds could prove useful in identifying cancer therapeutic agents. The interactions of the dimethyl-DAPP^{2+} dication with DNA have been investigated[40,41] previously, and there have been indications[40,41] that this dication can intercalate DNA, with a preference for G-C pairs over the A-T pairs. Additionally, it has been demonstrated[40] that dimethyl-DAPP^{2+} can be used as a selective fluorophore to detect A- and T-rich single-stranded polynucleotides, as well as having the potential to act as a sequence-specific artificial photonuclease.

To the best of our knowledge, no cancer cell proliferation studies have been carried out on the DAPP^{2+} dication, yet perylene analogues have been tested[42] for DNA telomerase inhibition while the structurally
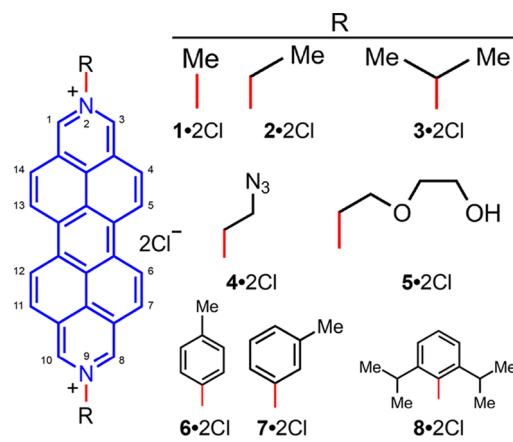

Figure 1. Structural formulas for the DAPP^{2+} 1·2Cl−8·2Cl derivatives that have been screened for anticancer activity. Numbering on the general structural formula indicates the substitution position on the DAPP^{2+} dication.

related diazapyrenium dications have been reported[43−45] to have encouraging therapeutic properties. 4,9-Diazapyrenium dications have been shown[43−45] to be able to intercalate DNA, and cancer-cell proliferation investigations have been carried out against human malignant MiaPaCa 2 (pancreatic), and Hep 2 (laryngeal) cell lines, in addition to the normal human fibroblast WI-38 cell line using two derivatives of these dications. It was found[45] that treatment of these cell lines with 4,9-diazapyrenium derivatives, in concentrations ranging from 100 nM to 100 μM, resulted in growth inhibition in excess of 50%, as well as their being more specific against the cancer cell lines than the WI-38 cell line. Additionally, the 2,7-diazapyrenium dication has been demonstrated[46] to undergo photochemical clevage of both supercoiled DNA pBR322 and DNA M13mp19.

Given the anticancer activity of the diazapyrenium dications, we might expect that the DAPP^{2+} dications would also possess anticancer activity, and may be more effective intercalators than the diazapyrenium dications on account of their extended polyaromatic cores. In our research on these dications, we sought to test the anticancer activity of a library of compounds. Since small structural variations may result in substantial differences in therapeutic activity and, given the fact that the dimethyl-DAPP^{2+} dication is capable of homophilic recognition, we synthesized a small library of compounds which can influence directly the way in which the dications interact with each other in solution. A cell proliferation assay was run in order to test the activity of each member of the library and we discovered that one candidate in particular has promising efficacy. Additionally, we have tested the efficacy of DAPP^{2+}-related compounds with different levels of aromaticity and found that there is a considerable difference between the potency of the completely aromatic diazaperopyrenium dications and the

hexahydroanthradiisoquinoline dications, which have less aromaticity, with the same functional groups on the 2 and 9 positions.

RESULTS AND DISCUSSION

Eight different DAPP^{2+} dications $\mathbf{1}^{2+}$–$\mathbf{8}^{2+}$ were synthesized with a range of different substituents on the nitrogens. Modification of these substituents changes the manner in which the dications aggregate in solution and in the solid state. This difference in packing has been observed[47−52] previously for perylene diimides, where the presence of large substituents on the imide nitrogens limit $\pi\cdots\pi$ aggregation without influencing the planarity of the central perylene core. Although substitution on the bay (5, 6, 12, and 13, Figure 1) positions of perylene diimides also limits[50,53−56] $\pi\cdots\pi$ aggregation, this substitution pattern results in conformational twisting of the perylene core. The eight different DAPP^{2+} dications were prepared by difunctionalization of the nitrogens located at the 2 and 9 positions. This protocol enables the preparation of the dichloride salts (Figure 1) where R = Me ($\mathbf{1}\cdot2Cl$), Et ($\mathbf{2}\cdot2Cl$), iPr ($\mathbf{3}\cdot2Cl$), $N_3CH_2CH_2$ ($\mathbf{4}\cdot2Cl$), $HOCH_2CH_2OCH_2CH_2$ ($\mathbf{5}\cdot2Cl$), p-MeC$_6$H$_4$ ($\mathbf{6}\cdot2Cl$), m-MeC$_6$H$_4$ ($\mathbf{7}\cdot2Cl$), and 2,6-iPr$_2$C$_6$H$_3$ ($\mathbf{8}\cdot2Cl$). These N-substituents were chosen for their ability to influence the way in which the dications pack in the solid state. We suspect that this packing most likely corresponds to the way in which these molecules aggregate in aqueous solutions.

Recently, we reported[36] the solid-state structure of the 2,9-dimethyl-DAPP^{2+} dication $\mathbf{1}^{2+}$, revealing that the dications pack in such a way as to form one-dimensional stacks. In this geometry, the perylene core of one dication is available to take part in $\pi\cdots\pi$ interactions with the perylene core of two neighboring dications which stack in a repetitive ABC manner so that the angle of N−N vectors between adjacent dications is approximately 60°, presumably to minimize Coulombic repulsions while maximizing $\pi\cdots\pi$ overlaps. Dication $\mathbf{5}^{2+}$ also displays (Figure 2) this particular solid-state packing behavior, where the angles between N−N vectors on the adjacent DAPP^{2+} dications are 63, 60 and 57°, and the interplanar spacings (centroid-to-centroid distances) are 3.57, 3.62, and 3.53 Å between neighboring perylene cores. In addition to the $\pi\cdots\pi$ interactions between these DAPP^{2+} dications, there are also multiple [C−H···O] interactions between (i) the protons α to the nitrogens and the terminal oxygen atoms in the diethylene glycol chains of adjacent DAPP^{2+} dications (3.11−3.38 Å), and (ii) the protons α to the nitrogens and the central oxygen atoms in the chains on the same DAPP^{2+} dication (2.91−3.35 Å). The [O···O] distance (2.76 Å) between terminal hydroxyl groups on adjacent DAPP^{2+} dications (Figure 2a) also constitutes yet another hydrogen bonding interaction present within
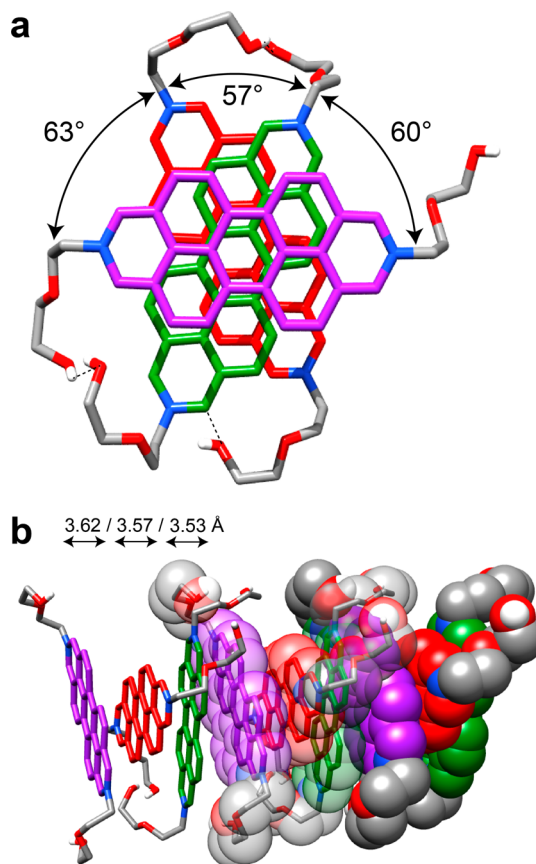

Figure 2. Solid-state superstructure of 5^{2+} displaying an ABC-type packing motif along one dimension. (a) Top-down view (tubular representation) of a single ABC stack showing the angles between the N−N vectors of adjacent 5^{2+} dications and multiple [C−H···O] and hydrogen bonding interactions, indicated by dashed lines. (b) Tubular and space-filling representation of three repeating ABC stacks shown with the centroid-to-centroid distances between adjacent dications.

the dicationic stacks. This combination of $\pi\cdots\pi$ stacking and hydrogen bonding interactions is reminiscent of a similar phenomenon observed[57] recently in single-crystals of all-organic materials possessing ferroelectric properties at room temperature.

When sterically more bulky substituents are present at the 2 and 9 positions of the DAPP^{2+} dications, the way in which those dications interact with one another to form one-dimensional stacks in the solid state changes to that of an AB stacking motif, $e.g.$, in the case of $\mathbf{3}^{2+}$, $\mathbf{6}^{2+}$, and $\mathbf{7}^{2+}$, with iPr, p-MeC$_6$H$_4$, and m-MeC$_6$H$_4$ substituents, respectively, the angles (Figure 3a,c,e) between the N−N vectors of adjacent DAPP^{2+} dications are 114.8, 112.8 and 119.7°, respectively. The presence of even bulkier groups, namely, 2,6-iPr$_2$C$_6$H$_3$, at the 2 and 9 positions of a DAPP^{2+} dication ($\mathbf{8}^{2+}$), imposes steric restrictions which inhibit $\pi\cdots\pi$ stacking interactions altogether. The solid-state structure (Figure 4) reveals that the isopropyl groups extend beyond the perylene core of the DAPP^{2+} dication, thereby blocking access to the perylene core by an adjacent dication. The planes of the 2,6-diisopropylphenyl
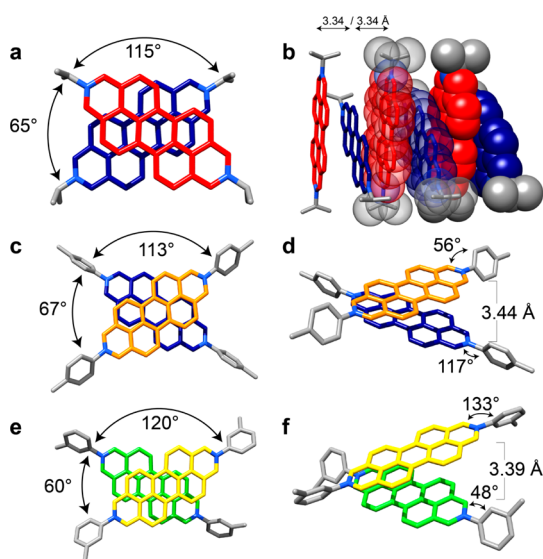
Figure 3. Tubular (and space-filling) representations of the solid-state superstructures revealing the angle and distance between adjacent dications for 3^{2+} (a and b), 6^{2+} (c and d), and 7^{2+} (e and f). All three dications display an ABAB stacking motif in the solid state as a result of the increased steric interactions provided by the substituents in the 2 and 9 positions of the diazaperopyrenium dication. For the numbering of the positions on the dication, please refer to the general structural formula in Figure 1.
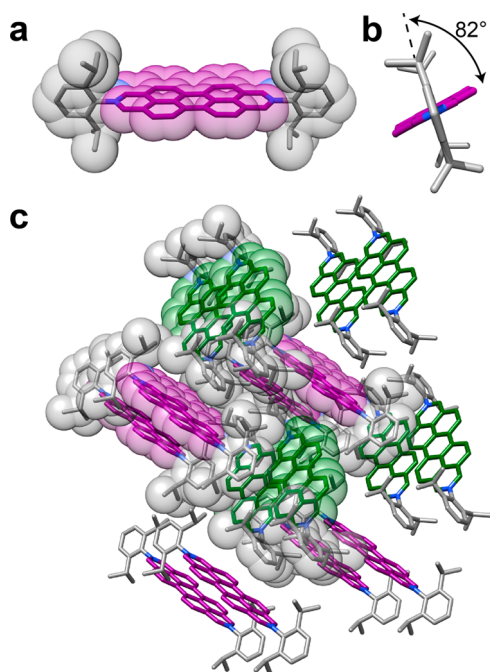

Figure 4. (a) Space-filling and tubular representations of the solid-state structure of 8^{2+} revealing that the isopropyl groups extend over the perylene core of the dication, inhibiting $\pi\cdots\pi$ stacking of these dications along one dimension. (b) View down the N–N vector of a single 8^{2+} dication revealing the angle between the plane of the diazaperopyrenium unit and the 2,6-diisopropylphenyl substituents located in the 2 and 9 positions of the dication. (c) Tubular (and space-filling) representations of the solid-state superstructure of 8^{2+} revealing a herringbone-like packing motif and the absence of any $\pi\cdots\pi$ interactions. Purple and green denote dications that are orientated in the same direction.

groups are nearly perpendicular (82°) to the DAPP^{2+} plane and result in the dications packing in a herringbone-like fashion. The presence of the two 2,6-iPr$_2$C$_6$H$_3$ groups also increases the solubility of the DAPP^{2+} dication in aqueous and polar organic solvents using chloride or hexafluorophosphate anions, respectively, compared to other groups, *e.g.*, as in the p-MeC$_6$H$_4$ and m-MeC$_6$H$_4$ derivatives, on account of the restricted ability of these dications to aggregate, a phenomenon which is also observed[47−52] with the related perylene diimides in organic solvents.

Given the facts (i) that DNA intercalators are common targets[58] for therapeutic development, (ii) that structurally similar pyrenium cations have demonstrated[43−45] anticancer activity, and (iii) that 2,9-dimethyl-DAPP^{2+} (1^{2+}) intercalates[40,41] ds-DNA, we sought to investigate the therapeutic potential of the range of DAPP^{2+} dications reported in this communication.

The antiproliferative effects of the dichloride salts of the DAPP^{2+} dications 1^{2+}−8^{2+} were evaluated against 10 cancerous cell lines—HT29 (colon), SKMEL-2 (melanoma), HepG2 (liver carcinoma), Jurkat (lymphoma), Hela (cervical), MDA-MB-231 (breast), PC-3 (prostate), FaDu (squamous cell carcinoma), HT-1080 (fibrosarcoma), and HL60 (leukemia). The antiproliferative screens were performed using a concentration of 10 μM of each of the dichlorides, with doxorubicin plated as a standard for comparison. The results, which are illustrated in Figure 5, are listed (Table S1) in detail in the Supporting Information. A number of the dichlorides resulted (shown as a dotted line in Figure 5) in lower than 50% viability after a 48 h incubation. Notably, the DAPP^{2+} dications 1^{2+}, 2^{2+} and 5^{2+} resulted in less than 50% cell survival, *i.e.*, 27.8 ± 0.8, 49.5 ± 2.3, 44.9 ± 2.5% cell viability, respectively, against HepG2 liver carcinoma cells, a statistically significant difference when compared to cells treated with doxorubicin with a cell viability of 74.9 ± 1.0%. The DAPP^{2+} dication 3^{2+}, which demonstrated a considerable antiproliferative effect (42.9 ± 1.9% cell viability) on HT-1080 fibrosarcoma cells, proved to be more potent than treatment with doxorubicin with a cell viability of 56.3 ± 5.5%. The most remarkable findings from the cell proliferation screen, however, were observed for the 2,9-bis(2,6-diisopropylphenyl)-DAPP^{2+} dication 8^{2+}. The dichloride $8\cdot$2Cl exhibited significant potency with less than 50% cell viability, against all but two of the cell lines tested, with the SKMEL-2 cell line having the lowest cell viability (7.2 ± 2.5%) when exposed to 10 μM of $8\cdot$2Cl. The data in Table 1 and the histogram illustrated in Figure 5a reveal six cell lines in which $8\cdot$2Cl had close to the same, or greater, potency as doxorubicin. These encouraging results prompted us to (i) investigate the anticancer activity of $8\cdot$2Cl further by performing a proliferation assay at various concentrations of the salt and (ii) generate
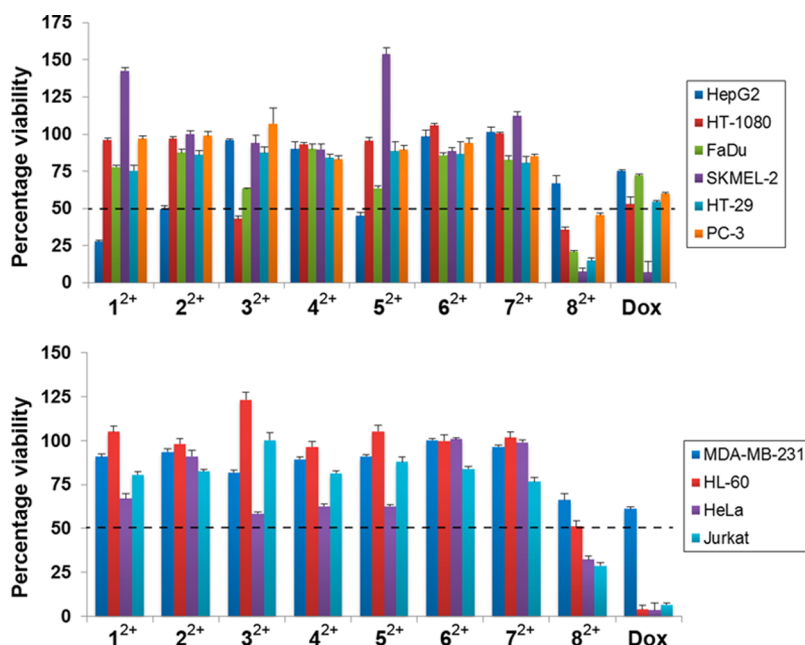
Figure 5. Effect on cell proliferation of each compound 1^{2+}–8^{2+} (as their dichlorides) and doxorubicin at 10 μM was evaluated against 10 cancer cell lines. (a) The six cell lines for which 8^{2+} had a similar efficacy to doxorubicin. (b) The four cell lines for which 8^{2+} was not as potent as doxorubicin. All dications were investigated as their chloride salts.

TABLE 1. Cell Viability Data for Compound 8·2Cl and Doxorubicin for the 10 Cell Lines Tested

	cell viability (%)	
cell line	8·2Cl	doxorubicin
FaDu	20.6 ± 1.1	72.2 ± 0.9
SKMEL-2	7.2 ± 2.5	6.9 ± 7.3
HT-29	14.9 ± 1.7	54.3 ± 0.9
HT-1080	35.6 ± 1.8	56.3 ± 5.5
HepG2	66.8 ± 5.2	74.9 ± 1.0
HL-60	51.1 ± 3.4	4.0 ± 2.5
Jurkat	28.9 ± 1.9	6.7 ± 0.9
PC-3	45.6 ± 1.2	59.7 ± 1.1
HeLa	32.3 ± 1.8	3.9 ± 4.0
MDA-MB-231	66.1 ± 3.5	61.1 ± 1.3

TABLE 2. IC50 Values Determined from Dose-Response Curves for 8·2Cl against Three Cell Lines

cell line	8·2Cl IC$_{50}$ (μM)
HT-29	0.51 ± 0.26
FaDu	4.81 ± 0.16
SKMEL-2	12.32 ± 0.19

dose−response curves. IC$_{50}$ values were derived from dose−response curves at nine different concentrations. The three cell lines HT-29, SKMEL-2, and FaDu, against which **8**·2Cl showed the highest toxicity from the proliferation screen, were tested. The resulting IC$_{50}$ values are listed in Table 2. Low micromolar efficacies of 12.3 ± 0.2 and 4.81 ± 0.2 μM were observed against SKMEL-2 and FaDu cells, respectively, while submicromolar potency (510 ± 260 nM) was observed with the HT-29 cell line.

We hypothesize that it is the propensity of the DAPP^{2+} salts to self-aggregate and the availability of the perylene core to take part in π···π or hydrophobic interactions which affects the potency of the compounds as cancer therapeutic agents when testing a library of these compounds. We recall that the packing in the solid state of the DAPP^{2+} dications 1^{2+} through

7^{2+} all show that π···π stacking interactions play a significant role in driving molecular orientation in their crystalline states. It is also reasonable to conclude that a hydrophobic effect operates in aqueous solution. When these π···π intermolecular interactions are inhibited by steric shielding of the diazaperopyrenium cores, the solution-phase molecules more likely exist in a monomeric state or at least as fleeting and small aggregates. This situation is reflected in the crystal packing (Figure 4) of the 8^{2+} dications wherein long-range, repetitive π···π associations between diaza-peropyrenium cores are impeded. These salts may be better suited to transitioning across membrane barriers or intercalating more efficiently than the aggregated species, leading to a marked increase in cell growth inhibition, as demonstrated by the higher potency of **8**·2Cl relative to the other DAPP^{2+} salts tested.

Dynamic light scattering (DLS) experiments were conducted on **1**·2Cl, **3**·2Cl, **5**·2Cl and **8**·2Cl to determine if the different DAPP^{2+} salts undergo solvent-directed aggregation in solution (see Supporting Information). In aqueous solution, **8**·2Cl was observed to form small (50−100 nm) stable aggregates, while **1**·2Cl and **3**·2Cl were observed to form only large

(>200 nm) aggregates that increase in diameter over time. Interestingly, $5 \cdot 2Cl$ was not observed to aggregate in deionized water, but aggregated over time in pH 7.2 phosphate-buffered solution. All samples tested in RPMI 1640 medium containing 5% fetal bovine serum resulted in signals greater than 100 nm, giving strong evidence to support the claim that the $DAPP^{2+}$ aggregation observed in aqueous and pH 7.2 phosphate-buffered solutions extends to the biological medium.

There is evidence, however, to support the belief that the dicationic state of 8^{2+} also plays a significant role in determining the potency and pharmacokinetic behavior observed during the screening against cancer cells. In support of this possibility we prepared compound 9 (Figure 6), namely, N,N-bis(2,6-diisopropylphenyl)perylene-3,4:9,10-bis(dicarboximide), which was also screened against cancer cell lines. Although location of bulky substituents on the terminal nitrogens could prevent aggregation, the presence of the carboximides removes the possibility of the formation of dications. This constitution allowed us to observe the effect of charge on the chemotherapeutic potency, while still maintaining some of the general structural ingredients of 8^{2+}. It transpires that the two 2,6-$iPr_2C_6H_3$ groups in 9 enhance its solubility in Me_2SO, by comparison with other perylene diimides with less bulky substituents. Of the 10 cell lines screened, all but one showed cell viability greater than 80%, suggesting that 9 is not as

effective a potential chemotherapeutic drug target as $8 \cdot 2Cl$. Compound 9 displayed (Table 3) relatively high potency ($26.3 \pm 9.5\%$ cell viability) against the HL-60 cell line, and, as such is significantly more effective ($51.1 \pm 3.4\%$ cell viability) than 8^{2+} for this particular cell line. The positive charge on 8^{2+}, as well as on $1^{2+}-7^{2+}$, most likely plays a crucial role in determining the effectiveness of these polyaromatic compounds as chemotherapeutic agents. The charged state could contribute to both the strengthening of the DNA intercalating ability of the $DAPP^{2+}$ dications as well as to increasing the probability of transition of the drug from the lipophilic membrane into the hydrophilic cytosol or nucleus. However, as we observed with HL-60, where 9 is more cytotoxic than $8 \cdot 2Cl$, there appears to be no universal characteristic associated with these compounds that suggests treatment of all cancer cell lines.

In order to investigate the nature of the structural effects of the $DAPP^{2+}$ dications in more detail, the degrees of aromaticity in the case of two of the dications were altered. In many drugs, the presence[59] of a basic amino group changes their solublities and pharmacodynamics properties, as well as providing some degree of lysosomotropic ability.[60−62] The library of structures examined so far in this investigation has focused on a possible correlation between $\pi \cdots \pi$ stacking propensity and therapeutic activity. Since failing to oxidize the "deoxygenated perylene diimide" intermediate at the final stage in synthesis leaves us with a protonatable amine derivative, it was of interest to test the therapeutic behavior of the basic amine as well as the change in the aromaticity in these compounds on cell viability. $A \cdot 2Cl$ and $B \cdot 2Cl$, derivatives of $3 \cdot 2Cl$ and $5 \cdot 2Cl$, respectively, were obtained as a result of not exposing the "deoxygenated perylene diimide" intermediate to the final oxidative dehydrogenation conditions, and thus the terminal heterocyclic rings are no longer aromatic in these structures (Figure 6). Although a comparison of cell viability between the diazaperopyrenium and hexahydroanthradiisoquinoline aromatic salts revealed similar cytotoxicities for most of the cell lines tested, $A \cdot 2Cl$ (Figure 7, Table 3)
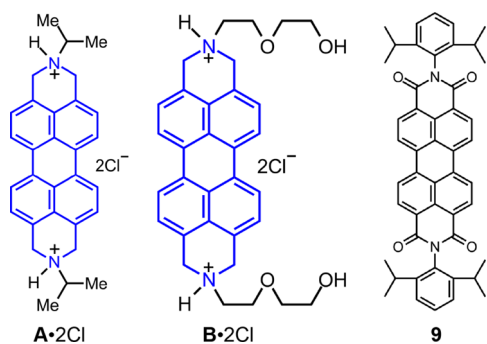

Figure 6. Structural formulas for compounds $A \cdot 2Cl$, $B \cdot 2Cl$, and 9.
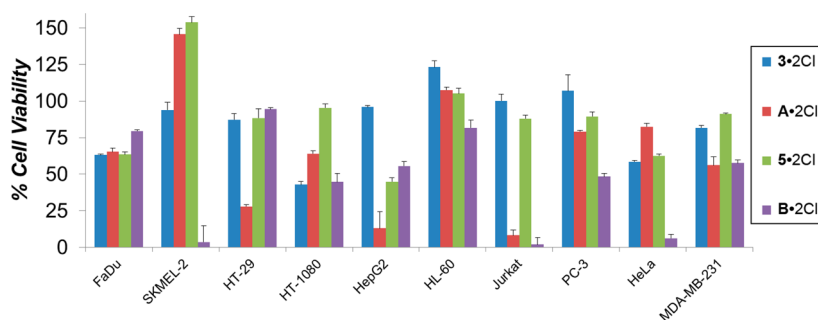
Figure 7. Comparison of cell viablilty between compounds $3 \cdot 2Cl$ and $5 \cdot 2Cl$ and their respective nonoxidized derivatives $A \cdot 2Cl$ and $B \cdot 2Cl$. For SKMEL-2, HT-29, HepG2, Jurkat and HeLa cell lines, there is a considerable difference in the potency of the dications based solely on the degree of aromatization.

TABLE 3. Cell Viability Data for A·2Cl, B·2Cl and 9 for the 10 Cell Lines Tested

	cell viability (%)		
cell line	A·2Cl	B·2Cl[a]	9[b]
FaDu	65.4 ± 2.5	79.6 ± 0.6	96.5 ± 0.6
SKMEL-2	145.7 ± 3.8	3.6 ± 11.1	106.2 ± 9.9
HT-29	28.0 ± 1.2	94.4 ± 1.0	92.4 ± 3.1
HT-1080	64.1 ± 1.9	44.7 ± 5.7	115.5 ± 1.6
HepG2	13.1 ± 11.3	55.5 ± 3.3	85.8 ± 1.4
HL-60	107.5 ± 2.0	81.8 ± 5.2	26.3 ± 9.5
Jurkat	8.3 ± 3.5	1.9 ± 4.7	85.6 ± 1.2
PC-3	79.1 ± 0.8	48.4 ± 2.2	88.2 ± 1.9
HeLa	82.5 ± 2.3	6.2 ± 2.8	94.7 ± 1.3
MDA-MB-231	56.2 ± 5.7	57.6 ± 2.0	98.0 ± 0.4

[a] Normalized to pure H_2O control. [b] Normalized to pure DMSO control.

appears to be more cytotoxic than the diazaperopyrenium salt **3**·2Cl in the HT-29, HepG2 and Jurkat cell lines. IC_{50} data for **A**·2Cl reveal low micromolar efficacy (1.3 ± 0.11 and 8.6 ± 0.17 μM) toward HepG2 and Jurkat cell lines, respectively, and submicromolar efficacy (620 ± 78 nM) against HT-29. Likewise, **B**·2Cl has greater cytotoxicity in the SKMEL-2, Jurkat, and HeLa cell lines than **5**·2Cl, with IC_{50} data indicating low micromolar efficacy (9.2 ± 7.1, 5.2 ± 0.18, and 1.8 ± 0.08 μM, respectively) against these cell lines. For both compounds, the IC_{50} values are comparable to those obtained with the doxorubicin controls. The concept of tuning aromaticity in polycyclic aromatic compounds could be a strategy worthy of further investigation for altering the toxicity behavior in this class of compounds.

CONCLUSION

We have demonstrated that a range of $DAPP^{2+}$ dications as their dichloride salts are potent chemotherapeutic targets. Modifying the nature and size of substituents on the 2 and 9 positions of the $DAPP^{2+}$ dication allows the potency toward specific cell lines to be tuned. The introduction of sterically demanding substitutents into these positions aids solubility in aqueous media and, in the case of **8**·2Cl, increases the potency against the majority of cell lines tested, particularly against HT-29, FaDu and SKMEL-2. Tailoring the aromaticity of the terminal heterocycles in these materials results in significant changes in the potency of the dications toward specific cell lines, particularly SKMEL-2, HepG2, Jurkat and HeLa. This investigation opens up another possible route toward the design and synthesis of new drug candidates for the treatment of cancer. Moreover, the unique spectroscopic properties[38−41] of these compounds could be employed to track their intracellular fate as well as to explore their mechanisms of action, in conjunction with photodynamic therapeutic techniques.

METHODS

Crystal Growth. Single crystals of suitable quality for single crystal X-ray diffraction were grown by the diffusion of iPr_2O vapor into MeCN solutions of **3**·2PF_6, **6**·2PF_6, and **7**·2PF_6. Likewise, good quality single crystals of **5**·2PF_6 and **8**·2PF_6 were grown by defusing a mixture of iPr_2O and Et_2O vapor into $MeNO_2$ and MeCN solutions, respectively.

Crystal Data. **3**·2PF_6: $2(C_{30}H_{26}N_2)$, $4(PF_6)$, C_2H_3N, orange needles, $M = 1449.99$, crystal size $0.244 \times 0.033 \times 0.016$ mm, orthorhombic, space group $Cmca$, $a = 6.6904(6)$, $b = 24.950(2)$ Å, $c = 35.310(3)$ Å, $\alpha = \beta = \gamma = 90°$, $V = 5894.1(9)$ Å^3, $\rho_{calc} = 1.634$, $T = 100(2)$ K, $Z = 4$, $R_1(F^2 > 2\sigma F^2) = 0.0844$, $wR_2 = 0.2037$. Out of 7618 reflections a total of 1717 were unique. **5**·2PF_6: $3(C_{32}H_{30}N_2O_4)$, $6(PF_6)$, $2(CH_3NO_2)$, orange needles, $M = 2511.64$, crystal size $0.409 \times 0.059 \times 0.04$ mm, monoclinic, space group Cc, $a = 35.4484(13)$, $b = 10.5194(4)$ Å, $c = 29.0669(10)$ Å, $\alpha = \gamma = 90°$, $\beta = 109.864(2)°$, $V = 10194.0(7)$ Å^3, $\rho_{calc} = 1.637$, $T = 100(2)$ K, $Z = 4$, $R_1(F^2 > 2\sigma F^2) = 0.0539$, $wR_2 = 0.1372$. Out of 24977 reflections a total of 24977 were unique. **6**·2PF_6: $2(C_{38}H_{26}N_2)$, $4(PF_6)$, $4.33(C_2H_3N)$, orange needles, $M = 1778.71$, crystal size $0.414 \times 0.037 \times 0.021$ mm, tetragonal, space group $P4/n$, $a = b = 34.0574(17)$ Å, $c = 6.9475(5)$ Å, $\alpha = \beta = \gamma = 90°$, $V = 8058.5(10)$ Å^3, $\rho_{calc} = 1.466$, $T = 100.01$ K, $Z = 4$, $R_1(F^2 > 2\sigma F^2) = 0.0773$, $wR_2 = 0.1879$. Out of 30323 reflections a total of 5798 were unique. **7**·2PF_6: $2(C_{38}H_{26}N_2)$, $4(PF_6)$, $5(C_2H_3N)$, orange needles, $M = 1806.36$, crystal size $0.203 \times 0.031 \times 0.027$ mm, monoclinic, space group $P2_1/c$, $a = 7.3021(3)$, $b = 13.6827(5)$ Å, $c = 39.2653(13)$ Å, $\alpha = \gamma = 90°$, $\beta = 95.246(2)°$, $V = 3906.7(3)$ Å^3, $\rho_{calc} = 1.536$, $T = 100(2)$ K, $Z = 2$, $R_1(F^2 > 2\sigma F^2) = 0.0700$, $wR_2 = 0.1825$. Out of 20840 reflections a total of 5587 were unique. **8**·2PF_6: $C_{48}H_{46}N_2$, $2(PF_6)$, $2(C_2H_3N)$, orange blocks, $M = 1022.91$, crystal size $0.66 \times 0.387 \times 0.214$ mm, monoclinic, space group $P2_1/c$, $a = 11.4221(4)$, $b = 13.2531(4)$ Å, $c = 15.8643(5)$ Å, $\alpha = \gamma = 90°$, $\beta = 99.1783(14)°$, $V = 2370.76(13)$ Å^3, $\rho_{calc} = 1.433$, $T = 100(2)$ K, $Z = 2$, $R_1(F^2 > 2\sigma F^2) = 0.0474$, $wR_2 = 0.1453$. Out of 101338 reflections a total of 11656 were unique. Crystallographic data (excluding structure factors) for the structures reported in this communication have been deposited with the Cambridge Crystallographic Data Center as supplementary publication nos. CCDC−1006815, 1006814, 1006817, 1006816, and 1006813, respectively.

Cell Studies. For cell studies, the hexafluorophosphate counterions were changed to chlorides by the addition of *n*-butyl ammonium chloride to acetonitrile solutions of the bis-(hexafluorophosphate)s. The resulting precipitate (the dichloride salt) was then collected and washed with acetonitrile to remove any excess of *n*-butyl ammonium chloride. The dichloride salts were then solubilized in a Me_2SO/H_2O mixture (50:50) to afford either 4 mM (**1**·2Cl, **3**·2Cl, **6**·2Cl, **7**·2Cl and **A**·2Cl) or 8 mM (compounds **2**·2Cl, **4**·2Cl, **5**·2Cl, **8**·2Cl and **B**·2Cl) solutions, which were subsequently used for cell viability studies. Compound **9** was solubilized in Me_2SO to produce an 8 mM solution that was used for cell viability studies. The growth inhibition of various cell lines was determined according to the protocols from the NCI/NIH Developmental Therapeutics Program, and in collaboration with the Northwestern University Developmental Therapeutics Core Facility. Cells were plated in triplicate in 96 well plates. The cells were plated at densities of 40 000 per well in 100 μL for suspended cells (Jurkat and HL-60) and 20 000 per well in 100 μL for adherent cells (HT-29, HT-1080, PC3, MDA-MB-231, FaDu, HepG2, Hela, SKMEL-2). The cells were grown in RPMI 1640 medium containing 5% fetal bovine serum and 2 mM L-glutamine. Following cell inoculation, the plates were incubated at 37 °C, 5% CO_2, 95% air and 100% relative humidity for 24 h.

After 24 h, the time-zero cells were fixed with ice cold trichloroacetic acid (TCA) (80% for suspended cells and 50% for adherent cells) and washed five times with water.

The compounds to be tested were diluted to twice the desired test concentration in complete media containing 50 μg/mL gentamicin. Aliquots of the compounds were added to the cells in a 1:1 volume ratio and the plates were incubated for an additional 48 h. The cells were then fixed using ice-cold trichloroacetic acid (TCA) (80% for suspended cells and 50% for adherent cells) and washed five times with water.

For the cell growth inhibition studies, the cells were stained by adding 100 μL of Sulphorhodamine B (SRB) solution (0.4% in 1% acetic acid) to each well, followed by incubation for 10 min at room temperature. The unbound dye was removed with five washes with 1% acetic acid, following which the plates were allowed to air-dry. The bound stain was solubilized for absorbance reading by adding 100 μL of 10 mM trizma (2-amino-2-(hydroxymethyl)-1,3-propanediol) base solution to each well, followed by absorbance reading at 490 nm with an automated plate reader (Synergy H1-M Microplate reader). The cell viability data reported was normalized to cell viability in an H_2O/DMSO 50:50 mixture unless otherwise stated. For half maximal inhibitory concentration studies, after fixing 100 μM Cell Titer Glo (Promega) was added to each well for 30 min. The wells were shaken for 2 min, followed by absorbance measurements.

Dynamic Light Scattering. The DAPP^{2+} salts were dissolved in H_2O/Me$_2$SO (1:1, v/v, 500 μL) to imitate the conditions used to introduce the sample to the cell cultures. Either deionized H_2O (1.0 mL), pH 7.2 phosphate buffered solution (1.0 mL) or the RPMI 1640 medium containing 5% fetal bovine serum and 2 mM L-glutamine (1.0 mL) was added to a Disposable Solvent Resistant Micro Cuvette (ZEN0040, Malvern). The DAPP^{2+} salt solution (10 μL) was then injected into the cuvette. Analyses of the samples were carried out on a Malvern Instruments Inc., Zetasizer Nano ZS. Measurements were taken using a standard operating procedure (SOP) (10 scans at 10 s/scan) for aqueous solutions at 25 °C. All solvents were run as blanks to identify peaks that correlate to the protein additives or possible impurities in solution.

Conflict of Interest: The authors declare no competing financial interest.

Supporting Information Available: Additional results, materials and general methods, NMR and DLS characterization. This material is available free of charge *via* the Internet at http://pubs.acs.org.

REFERENCES AND NOTES

1. Müller, W.; Crothers, D. M. Studies of the Binding of Actinomycin and Related Compounds to DNA. *J. Mol. Biol.* **1968**, *35*, 251–290.
2. Hurley, L. H. DNA and Its Associated Processes as Targets for Cancer Therapy. *Nat. Rev. Cancer* **2002**, *2*, 188–200.
3. Tewey, K.; Rowe, T.; Yang, L.; Halligan, B.; Liu, L. Adriamycin-Induced DNA Damage Mediated by Mammalian DNA Topoisomerase II. *Science* **1984**, *226*, 466–468.
4. Minford, J.; Pommier, Y.; Filipski, J.; Kohn, K. W.; Kerrigan, D.; Mattern, M.; Michaels, S.; Schwartz, R.; Zwelling, L. A. Isolation of Intercalator-Dependent Protein-Linked DNA Strand Cleavage Activity from Cell Nuclei and Identification as Topoisomerase II. *Biochemistry* **1986**, *25*, 9–16.
5. Henderson, D.; Hurley, L. H. Molecular Struggle for Transcriptional Control. *Nat. Med.* **1995**, *1*, 525–527.
6. Pohl, F. M.; Jovin, T. M.; Baehr, W.; Holbrook, J. J. Ethidium Bromide as a Cooperative Effector of a DNA Structure. *Proc. Natl. Acad. Sci. U. S. A.* **1972**, *69*, 3805–3809.
7. Heinen, E.; Bassleer, R.; Calberg-Bacq, C. M.; Desaive, C.; Lepoint, A. Comparative Study of the Effects of Ethidium Bromide and DNA-Ethidium Bromide Complex on Normal and Cancer Cells. *Biochem. Pharmacol.* **1974**, *23*, 1549–1551.
8. Sobell, H. M.; Reddy, B. S.; Bhandary, K. K.; Jain, S. C.; Sakore, T. D.; Seshadri, T. P. Conformational Flexibility in DNA Structure as Revealed by Structural Studies of Drug Intercalation and Its Broader Implications in Understanding the Organization of DNA in Chromatin. *Cold Spring Harbor Symp. Quant. Biol.* **1978**, *42*, 87–102.
9. Alonso, A.; Almendral, M. J.; Curto, Y.; Criado, J. J.; Rodríguez, E.; Manzano, J. L. Determination of the DNA-Binding Characteristics of Ethidium Bromide, Proflavine, and Cisplatin by Flow Injection Analysis: Usefulness in Studies on Antitumor Drugs. *Anal. Biochem.* **2006**, *355*, 157–164.
10. Greschner, A. A.; Bujold, K. E.; Sleiman, H. F. Intercalators as Molecular Chaperones in DNA Self-Assembly. *J. Am. Chem. Soc.* **2013**, *135*, 11283–11288.
11. Rescifina, A.; Zagni, C.; Varrica, M. G.; Pistarà, V.; Corsaro, A. Recent Advances in Small Organic Molecules as DNA Intercalating Agents: Synthesis, Activity, and Modeling. *Eur. J. Med. Chem.* **2014**, *74*, 95–115.
12. Lerman, L. S. Structural Considerations in the Interaction of DNA and Acridines. *J. Mol. Biol.* **1961**, *3*, 18–30.
13. Neidle, S.; Pearl, L. H.; Herzyk, P.; Berman, H. M. A Molecular Model for Proflavine–DNA Intercalation. *Nucleic Acids Res.* **1988**, *16*, 8999–9016.
14. Denny, W. A. Acridine Derivatives as Chemotherapeutic Agents. *Curr. Med. Chem.* **2002**, *9*, 1655–1665.
15. Sasikala, W. D.; Mukherjee, A. Molecular Mechanism of Direct Proflavine–DNA Intercalation: Evidence for Drug-Induced Minimum Base-Stacking Penalty Pathway. *J. Phys. Chem. B* **2012**, *116*, 12208–12212.
16. Jain, S. S.; LaFratta, C. N.; Medina, A.; Pelse, I. Proflavine–DNA Binding Using a Handheld Fluorescence Spectrometer: A Laboratory for Introductory Chemistry. *J. Chem. Educ.* **2013**, *90*, 1215–1217.
17. Emmanuel Saltiel, W. M. Doxorubicin (Adriamycin) Cardiomyopathy—A Critical Review. *West. J. Med.* **1983**, *139*, 332–341.
18. Bodley, A.; Liu, L. F.; Israel, M.; Seshadri, R.; Koseki, Y.; Giuliani, F. C.; Kirschenbaum, S.; Silber, R.; Potmesil, M. DNA Topoisomerase II-Mediated Interaction of Doxorubicin and Daunorubicin Congeners with DNA. *Cancer Res.* **1989**, *49*, 5969–5978.
19. Lipscomb, L. A.; Peek, M. E.; Zhou, F. X.; Bertrand, J. A.; VanDerveer, D.; Williams, L. D. Water Ring Structure at DNA Interfaces: Hydration and Dynamics of DNA-Anthracycline Complexes. *Biochemistry* **1994**, *33*, 3649–3659.
20. Gewirtz, D. A. A Critical Evaluation of the Mechanisms of Action Proposed for the Antitumor Effects of the Anthracycline Antibiotics Adriamycin and Daunorubicin. *Biochem. Pharmacol.* **1999**, *57*, 727–741.
21. Perego, P.; Corna, E.; Cesare, M. D.; Gatti, L.; Polizzi, D.; Pratesi, G.; Supino, R.; Zunino, F. Role of Apoptosis and Apoptosis-Related Genes in Cellular Response and Antitumor Efficacy of Anthracyclines. *Curr. Med. Chem.* **2001**, *8*, 31–37.
22. Cortés-Funes, H.; Coronado, C. Role of Anthracyclines in the Era of Targeted Therapy. *Cardiovasc. Toxicol.* **2007**, *7*, 56–60.
23. Rosell, R.; Carles, J.; Abad, A.; Ribelles, N.; Barnadas, A.; Benavides, A.; Martín, M. Phase I Study of Mitonafide in 120 h Continuous Infusion in Non-Small Cell Lung Cancer. *Invest. New Drugs* **1992**, *10*, 171–175.
24. Braña, M. F.; Ramos, A. Naphthalimides as Anticancer Agents: Synthesis and Biological Activity. *Curr. Med. Chem.: Anti-Cancer Agents* **2001**, *1*, 237–255.

25. Saez, R.; Craig, J. B.; Kuhn, J. G.; Weiss, G. R.; Koeller, J.; Phillips, J.; Havlin, K.; Harman, G.; Hardy, J.; Melink, T. J. Phase I Clinical Investigation of Amonafide. *J. Clin. Oncol.* **1989**, *7*, 1351–1358.

26. Braña, M. F.; Cacho, M.; García, M. A.; de Pascual-Teresa, B.; Ramos, A.; Domínguez, M. T.; Pozuelo, J. M.; Abradelo, C.; Rey-Stolle, M. F.; Yuste, M.; *et al.* New Analogues of Amonafide and Elinafide, Containing Aromatic Heterocycles: Synthesis, Antitumor Activity, Molecular Modeling, and DNA Binding Properties. *J. Med. Chem.* **2004**, *47*, 1391–1399.

27. Braña, M. F.; Castellano, J. M.; Moran, M.; Perez de Vega, M. J.; Romerdahl, C. R.; Qian, X. D.; Bousquet, P.; Emling, F.; Schlick, E.; Keilhauer, G. Bis-Naphthalimides: A New Class of Antitumor Agents. *Anti-Cancer Drug Des.* **1993**, *8*, 257–268.

28. Bousquet, P. F.; Braña, M. F.; Conlon, D.; Fitzgerald, K. M.; Perron, D.; Cocchiaro, C.; Miller, R.; Moran, M.; George, J.; Qian, X.-D.; *et al.* Preclinical Evaluation of LU 79553: A Novel Bis-Naphthalimide with Potent Antitumor Activity. *Cancer Res.* **1995**, *55*, 1176–1180.

29. Villalona-Calero, M. A.; Eder, J. P.; Toppmeyer, D. L.; Allen, L. F.; Fram, R.; Velagapudi, R.; Myers, M.; Amato, A.; Kagen-Hallet, K.; Razvillas, B.; *et al.* Phase I and Pharmacokinetic Study of LU79553, a DNA Intercalating Bisnaphthalimide, in Patients With Solid Malignancies. *J. Clin. Oncol.* **2001**, *19*, 857–869.

30. Bailly, C.; Carrasco, C.; Joubert, A.; Bal, C.; Wattez, N.; Hildebrand, M.-P.; Lansiaux, A.; Colson, P.; Houssier, C.; Cacho, M.; *et al.* Chromophore-Modified Bisnaphthalimides: DNA Recognition, Topoisomerase Inhibition, and Cytotoxic Properties of Two Mono- and Bisfuronaphthalimides. *Biochemistry* **2003**, *42*, 4136–4150.

31. de Isabella, P.; Zunino, F.; Capranico, G. Base Sequence Determinants of Amonafide Stimulation of Topoisomerase II DNA Cleavage. *Nucleic Acids Res.* **1995**, *23*, 223–229.

32. Avendaño, C.; Menéndez, J. C. DNA Intercalators and Topoisomerase Inhibitors. In *Medicinal Chemistry of Anticancer Drugs*; Avendaño, C., Menéndez, J. C., Eds.; Elsevier: Amsterdam, 2008; Chapter 7, pp 199–228.

33. Ingrassia, L.; Lefranc, F.; Kiss, R.; Mijatovic, T. Naphthalimides and Azonafides as Promising Anti-Cancer Agents. *Curr. Med. Chem.* **2009**, *16*, 1192–1213.

34. Gabbay, E. J.; Grier, D.; Fingerle, R. E.; Reimer, R.; Levy, R.; Pearce, S. W.; Wilson, W. D. Interaction Specificity of the Anthracyclines with Deoxyribonucleic Acid. *Biochemistry* **1976**, *15*, 2062–2070.

35. Kubař, T.; Hanus, M.; Ryjáček, F.; Hobza, P. Binding of Cationic and Neutral Phenanthridine Intercalators to a DNA Oligomer is Controlled by Dispersion Energy: Quantum Chemical Calculations and Molecular Mechanics Simulations. *Chem.—Eur. J.* **2006**, *12*, 280–290.

36. Basuray, A. N.; Jacquot de Rouville, H.-P.; Hartlieb, K. J.; Kikuchi, T.; Strutt, N. L.; Bruns, C. J.; Ambrogio, M. W.; Avestro, A.-J.; Schneebeli, S. T.; Fahrenbach, A. C.; *et al.* The Chameleonic Nature of Diazaperopyrenium Recognition Processes. *Angew. Chem., Int. Ed.* **2012**, *51*, 11872–11877.

37. Basuray, A. N.; Jacquot de Rouville, H.-P.; Hartlieb, K. J.; Fahrenbach, A. C.; Stoddart, J. F. Beyond Perylene Diimides—Diazaperopyrenium Dications as Chameleonic Nanoscale Building Blocks. *Chem.—Asian J.* **2013**, *8*, 524–532.

38. Hartlieb, K. J.; Basuray, A. N.; Ke, C.; Sarjeant, A. A.; Jacquot de Rouville, H.-P.; Kikuchi, T.; Forgan, R. S.; Kurutz, J. W.; Stoddart, J. F. Chameleonic Binding of the Dimethyldiazaperopyrenium Dication by Cucurbit[8]uril. *Asian J. Org. Chem.* **2013**, *2*, 225–229.

39. Sampath, S.; Basuray, A. N.; Hartlieb, K. J.; Aytun, T.; Stupp, S. I.; Stoddart, J. F. Direct Exfoliation of Graphite to Graphene in Aqueous Media with Diazaperopyrenium Dications. *Adv. Mater.* **2013**, *25*, 2740–2745.

40. Slama-Schwok, A.; Jazwinski, J.; Bere, A.; Montenay-Garestier, T.; Rougee, M.; Helene, C.; Lehn, J. M. Interactions of the Dimethyldiazaperopyrenium Dication with Nucleic Acids. 1. Binding to Nucleic Acid Components and to Single-Stranded Polynucleotides and Photocleavage of Single-Stranded Oligonucleotides. *Biochemistry* **1989**, *28*, 3227–3234.

41. Slama-Schwok, A.; Rougee, M.; Ibanez, V.; Geacintov, N. E.; Montenay-Garestier, T.; Lehn, J. M.; Helene, C. Interactions of the Dimethyldiazaperopyrenium Dication with Nucleic Acids. 2. Binding to Double-Stranded Polynucleotides. *Biochemistry* **1989**, *28*, 3234–3242.

42. Sissi, C.; Lucatello, L.; Krapcho, A. P.; Maloney, D. J.; Boxer, M. B.; Camarasa, M. V.; Pezzoni, G.; Menta, E.; Palumbo, M. Tri-, Tetra- and Heptacyclic Perylene Analogues as New Potential Antineoplastic Agents Based on DNA Telomerase Inhibition. *Bioorg. Med. Chem.* **2007**, *15*, 555–562.

43. Piantanida, I.; Palm, B. S.; Zinić, M.; Schneider, H.-J. A New 4,9-Diazapyrenium Intercalator for Single- and Double-Stranded Nucleic Acids: Distinct Differences from Related Diazapyrenium Compounds and Ethidium Bromide. *J. Chem. Soc., Perkin Trans. 2* **2001**, 1808–1816.

44. Piantanida, I.; Tomisic, V.; Zinić, M. 4,9-Diazapyrenium Cations. Synthesis, Physico-Chemical Properties and Binding of Nucleotides in Water. *J. Chem. Soc., Perkin Trans. 2* **2000**, 375–383.

45. Steiner-Biocić, I.; Glavas-Obrovac, L.; Karner, I.; Piantanida, I.; Zinić, M.; Pavelić, K.; Pavelić, J. 4,9-Diazapyrenium Dications Induce Apoptosis in Human Tumor Cells. *Anticancer Res.* **1996**, *16*, 3705–3708.

46. Blacker, A. J.; Jazwinski, J.; Lehn, J.-M.; Wilhelm, F. X. Photochemical Cleavage of DNA by 2,7-Diazapyrenium Cations. *J. Chem. Soc., Chem. Commun.* **1986**, 1035–1037.

47. Rademacher, A.; Märkle, S.; Langhals, H. Lösliche Perylen-Fluoreszenzfarbstoffe mit hoher Photostabilität. *Chem. Ber.* **1982**, *115*, 2927–2934.

48. Deyama, K.; Tomoda, H.; Muramatsu, H.; Matsui, M. 3,4,9,10-Perylenetetracarboxdiimides Containing Perfluoroalkyl Substituents. *Dyes Pigm.* **1996**, *30*, 73–78.

49. Langhals, H.; Ismael, R.; Yürük, O. Persistent Fluorescence of Perylene Dyes by Steric Inhibition of Aggregation. *Tetrahedron* **2000**, *56*, 5435–5441.

50. Weil, T.; Vosch, T.; Hofkens, J.; Peneva, K.; Müllen, K. The Rylene Colorant Family—Tailored Nanoemitters for Photonics Research and Applications. *Angew. Chem., Int. Ed.* **2010**, *49*, 9068–9093.

51. Ramanan, C.; Smeigh, A. L.; Anthony, J. E.; Marks, T. J.; Wasielewski, M. R. Competition between Singlet Fission and Charge Separation in Solution-Processed Blend Films of 6,13-Bis(triisopropylsilylethynyl)pentacene with Sterically-Encumbered Perylene-3,4:9,10-bis(dicarboximide)s. *J. Am. Chem. Soc.* **2011**, *134*, 386–397.

52. Frischmann, P. D.; Würthner, F. Synthesis of a Non-aggregating Bay-Unsubstituted Perylene Bisimide Dye with Latent Bromo Groups for C–C Cross Coupling. *Org. Lett.* **2013**, *15*, 4674–4677.

53. Würthner, F. Perylene Bisimide Dyes as Versatile Building Blocks for Functional Supramolecular Architectures. *Chem. Commun.* **2004**, 1564–1579.

54. Langhals, H. Control of the Interactions in Multichromophores: Novel Concepts. Perylene Bis-imides as Components for Larger Functional Units. *Helv. Chim. Acta* **2005**, *88*, 1309–1343.

55. Jung, C.; Ruthardt, N.; Lewis, R.; Michaelis, J.; Sodeik, B.; Nolde, F.; Peneva, K.; Müllen, K.; Bräuchle, C. Photophysics of New Water-Soluble Terrylenediimide Derivatives and Applications in Biology. *ChemPhysChem* **2009**, *10*, 180–190.

56. Huang, C.; Barlow, S.; Marder, S. R. Perylene-3,4,9,10-tetracarboxylic Acid Diimides: Synthesis, Physical Properties, and Use in Organic Electronics. *J. Org. Chem.* **2011**, *76*, 2386–2407.

57. Tayi, A. S.; Shveyd, A. K.; Sue, A. C. H.; Szarko, J. M.; Rolczynski, B. S.; Cao, D.; Kennedy, T. J.; Sarjeant, A. A.; Stern, C. L.; Paxton, W. F.; *et al.* Room-Temperature Ferroelectricity in Supramolecular Networks of Charge-Transfer Complexes. *Nature* **2012**, *488*, 485–489.

58. Palchaudhuri, R.; Hergenrother, P. J. DNA as a Target for Anticancer Compounds: Methods to Determine the Mode

of Binding and the Mechanism of Action. *Curr. Opin. Biotechnol.* **2007**, *18*, 497–503.

59. Goldman, S. D. B.; Funk, R. S.; Rajewski, R. A.; Krise, J. P. Mechanisms of Amine Accumulation in, and Egress from, Lysosomes. *Bioanalysis* **2009**, *1*, 1445–1459.

60. Binaschi, M.; Bigioni, M.; Cipollone, A.; Rossi, C.; Goso, C.; Maggi, C. A.; Capranico, G.; Animati, F. Anthracyclines: Selected New Developments. *Curr. Med. Chem.: Anti-Cancer Agents* **2001**, *1*, 113–130.

61. Gong, Y.; Duvvuri, M.; Duncan, M. B.; Liu, J.; Krise, J. P. Niemann-Pick C1 Protein Facilitates the Efflux of the Anticancer Drug Daunorubicin from Cells According to a Novel Vesicle-Mediated Pathway. *J. Pharmacol. Exp. Ther.* **2006**, *316*, 242–247.

62. Chen, V. Y.; Posada, M. M.; Blazer, L. L.; Zhao, T.; Rosania, G. R. The Role of the VPS4A-Exosome Pathway in the Intrinsic Egress Route of a DNA-Binding Anticancer Drug. *Pharm. Res.* **2006**, *23*, 1687–1695.